Nucleation-growth and diffusion processes studied by atomic force microscopy and nanoconductimetry

H. Di Murro[1], E. Lesniewska[2,] , E. Gallucci[3,] , D. Sorrentino[1], C. Vernet[1]

[1]Lafarge Centre de Recherche, Saint Quentin Fallavier, France;
[2] LPUB UMR CNRS 5027, University of Bourgogne, Dijon, France
[3] LMC, EPFL, Lausanne, Switzerland

Abstract

The processes of nucleation-growth and diffusion leading to the development of the microstructure of the cement pastes have been studied.
Atomic force microscopy was used to study representative phases of cement in order to investigate the early stages of hydration. In order to identify the different phases and their evolution in time, some complementary observations were performed on cement pastes by nanoindentation.
Recent developments in conductimetry at nanometer-scale resolution, allowed the study of the diffusion processes involved at the beginning of hydration. Binary and ternary subsystems based on mixtures of different components such as: C_3A, C_3S, and gypsum, were studied, with a view to understand the role of diffusional processes. The study brings new quantitative experimental elements, which can be incorporated, into the models of microstructure development.

Keywords: AFM, nanoindentation, nanoconductivity, nucleation, interaction, reactivity, alite, C_3A

1. Introduction

Hydraulic binders such as plaster or cement are the most widely used materials today. Microstructural studies of plaster and cement conducted over the past few decades have greatly influenced the way hydraulic binders are used. Theory and practice have advanced more or less in step, and we are now achieving real benefit from extending the length scale from macroscopic to the microscale level. Just as microstructural methods of cement characterisation have been successfully pursued over the past several decades, to the point where performance-related models increasingly incorporate microstructural features, we must also characterise, control and manipulate nanostructures to achieve advanced multifunctional materials. This will require a drastic extension of knowledge and a mastering of structure in heterogeneous materials at scales from nano- to macroscale. It will require fundamental advances in the physics and chemico-mechanics of non equilibrium dissolution, diffusion and crystal growth phenomena. Traditionally the properties of cement and concrete have been studied on a macroscopic basis. In comparison, advances in other structural materials, e.g., metals, ceramics, have been achieved by extending the scale of investigation from macroscopic to microscopic level and, ultimately, to the nanoscale level.

Since 1996, Atomic Force Microscopy (AFM) was used at the University of Bourgogne to image the surface reactivity as well as to characterize quantitatively the surface forces between gypsum crystals, the hydration product of plaster **[1, 2]**. Measurements on different crystal faces, which vary in morphology, structure, hydrophilicity, surface charge, were performed in both air and ionic solutions. In ionic solutions, varying the experimental parameters, the ionic nature and the concentration as well as the duration of the contact leads to the conclusion that the adhesion occurred whatever the orientation of faces **[3]**. Nevertheless, the magnitude of the adhesion of a physical nature Van der Waals and ionic correlation depends on the surface charge density of each face while its increase is related to the growth of the contact area between the two crystals. In air, the systematic determination of surface potential with respect to the orientation of crystalline faces, the relative humidity and the duration and the area of contact between gypsum crystals suggested three types of physical forces: the Van der Waals forces, the electrostatic and capillary forces. In addition, the reactivity study displayed a reactive process of matter transfer, which is added to the surface forces to ensure the adhesion. Correlation between AFM results related to the micrometer scale and rheological measurements, performed on plaster suspensions pastes and on macroscopic hardened plaster beams, was also demonstrated. Since 2000, the capacities of force detection of atomic force microscopy have been used in order to measure the interfacial forces between the main cement hydrate, e.g., calcium silicate hydrate (C-S-H) nanoparticles and try to understand the mechanisms who govern the hardening of cement **[4]**. The evolution of these forces is extensively dependent of the chemical activity of C-S-H **[5]**. A novel process of C-S-H synthesis permits for the first time, to identify the structure at the atomic scale of the C-S-H nanoparticles. The structure was found dependent on the calcium/silicon ratio **[6]**. The synthesized C-S-H crystals prove to be a model substrate for the investigation of the kinetics of adsorption of cement additives such as polymers.

From C-S-H models to the complexity of the mixtures within the cement pastes, a new stage is essential: the comprehension of the hydration of the other anhydrous phases before moving to binary system, ternary system...

In order to correlate the microstructural studies conducted on scanning electron microscopy (SEM) **[7]** or solid state nuclear magnetic resonance (NMR) **[8]** with our advanced practice at nanoscale investigation by atomic force microscopy (AFM), the research was focused on the diffusion processes occurring in cement paste. Characterization of the nanostructural features of cement will authorize the control of the setting and the formation of the matrix. The nanostructures manipulation will achieve advanced multifunctional materials.
In the present study, we propose to develop an experimental approach to compare microstructural and nanostructural investigation on multiphase material. We will present the first attempt to measure the diffusion process on surface in electrolytic solution.

2. Material and methods

2.1 Atomic force microscopy

All experiments were performed into a glove box free from carbon dioxide to prevent carbonation of hydroxide solutions. Inside, a multimode atomic force microscope (AFM) (Nanoscope IIIa Quadrex; Veeco Co., CA) equipped with different scanners (15-150 µm) was operated in contact mode. For studies in aqueous solutions, an adapted commercial fluid cell associated with a fluid exchange system was used to maintain steady bulk concentrations for all diffusion processes acting on the anhydrous grains. Equilibrated prepared calcium hydroxide solutions flowed through the fluid cell. The temperature of the surrounding wall was maintained at 25°C.
For morphological investigation, we have used V-shaped silicon nitride cantilevers or rectangular silicon cantilevers with spring constants of 10 - 600 mN/m measured by resonance frequency method and the noise measurement method.
For adhesion force measurement, we have used pyramidal silicon nitride Si_3N_4 probes associated to commercial cantilevers, double-side Au coated with a measured spring constant ranging of about 0.6-1 N/m (DNP nanoprobe; Veeco Co., CA), were used. C-S-H coverage was obtained by using the layer of silica as substrate for calcium silicate hydrates growth in saturated calcium hydroxide solution. Under these conditions, C-S-H precipitates on the tip apex from the silicate ions provided by the dissolution of silica in the alkaline medium and from the calcium and hydroxide ions from the solution. After complete consumption of the silica layer, the probe was also rendered non-reactive, as long as the silicon nitride bulk was preserved from oxidation (coverage checked for each probes batch). Concerning the force measurement in solution, the rate of the vertical motion performed during the approach-retract cycles was lowered to 50 $nm.s^{-1}$ in order to avoid changing the viscosity of the medium. The force versus separation curves were limited to the range 0-25 nm. However, in each case first measurements were performed with larger displacements (250 nm). The first retract curves was also recorded. In these conditions, the C-S-H probe and the substrate were kept in contact two seconds. The maximum force applied by the cantilever reaches 10-20 nN. For each experiment, statistics of over 100 force measurements per sample were established by recording 4 force curves on 25 different locations from each sample (force volume mapping). Five samples were analyzed for each different configuration.
Concerning nanoindentation experiments, we have used rectangular stainless steel cantilevers (DNISP nanoindentation probe; Veeco Co., CA) associated to a diamond probe with a radius of curvature at the apex of about 25 nm. The cantilever spring constant was about 210 N/m, measured by resonance frequency method (64 kHz,

sensitivity 176 nm/V used for spring constant calibration). The typical depth of the indentation was less than 10 nm.

2.2 C_3A Synthesis

C_3A phase has an important reactivity. This phase is generally in the cement and clinker in amount of 5-10%. To prepare the C_3A with a cubic structure, it was necessary to mix Al_2O_3 and $CaCO_3$ homogeneously respectively with the quantity of 62.54% and 37.8% **[9]**. The mix was grounded with water during 1h30 to obtain a homogeneous paste. After, the mix was heated at 950°C during 1h to decarbonate $CaCO_3$ of the mix, and then at 1450°C during 4h. The quality of the end product was controlled by chemical analysis such as by X-rays diffraction, X-ray fluorescence, and dosage with glycol of free lime to know precisely the purity. The XRD diffractograms showed that tricalcium aluminate was relatively pure (i.e. CaO peak located at 54° angle missed). Moreover we have observed that C_3A was cubic form. The analysis by X-ray fluorescence showed by calculation that tricalcium aluminate had a molar ratio of $CaO/(Al_2O_3 + F_2O_3)$ equal to 2.99±0.001. Iron was substituted to aluminum in the C_3A network. The ratio was close to theoretical stoichiometry. Dosage of free lime by glycol indicated purity higher than 97.4%±0.38% (without taking into account the C_3A value partially dissolved in glycol during the dosage).

2.3 Alite synthesis

The alite, crystallize in triclinic T or a monoclinic M1, M2, M3 forms **[10]** in function of the impurities concentration in the unit cell. The alite in clinker is present generally in form of a mix of M1 + M3 forms. The synthesis of C_3S was obtaining by burning the main components using alite formula: C_3S + 0.9% Al_2O_3 + 0.6% MgO **[10]**. To prepare the alite phase, it was necessary to mix $CaCO_3$ (81.69%), SiO_2 (16.41%), MgO (1.27%) and Al_2O_3 (0.627%) homogeneously **[11]**. The mix was grounded with water during 1h30 to obtain a homogeneous paste. After the mix was heated at 950°C during 1h to decarbonate $CaCO_3$ of the mix, and then at 1600°C during 4h. After that it was necessary to verify the purity of the product and the phase structure with XRD and dosage in the glycol. The value of the percentage of the free lime in the Alite is 0.2 ±0.07%.

3. Results and discussion

3.1 Study of the hydration of the pure cement phase

The different synthesized cement phases, were observed by atomic force microscopy First of all the surface reactivity of the sample was observed during the hydration and then the evolution of the adherence force between C-S-H and C_3S, between C-S-H and C_2S and finally between AH_3 ($Al_2(OH)_6$) and C_3A in the 3 systems studied.

Hydration of C_3S in calcium hydroxide solution

The evolutions of the adhesion force between the C-S-H and C_3S in saturated calcium hydroxide solution (22 mmol/L) are represented in figure 1.

All C_3S samples having a closer specific volume, force measurements were correlated with the images obtained at the time of the kinetics of hydration of tricalcium silicate (Fig. 1).

In the insets, representative images (2 µm diameter size) are shown taken with standard Si_3N_4 probes. The evolution of the force between C-S-H coated probe and C_3S sample is correlated to the topographical kinetics (i.e. growth of hydrates: portlandite and calcium silicate hydrates reported in insets).

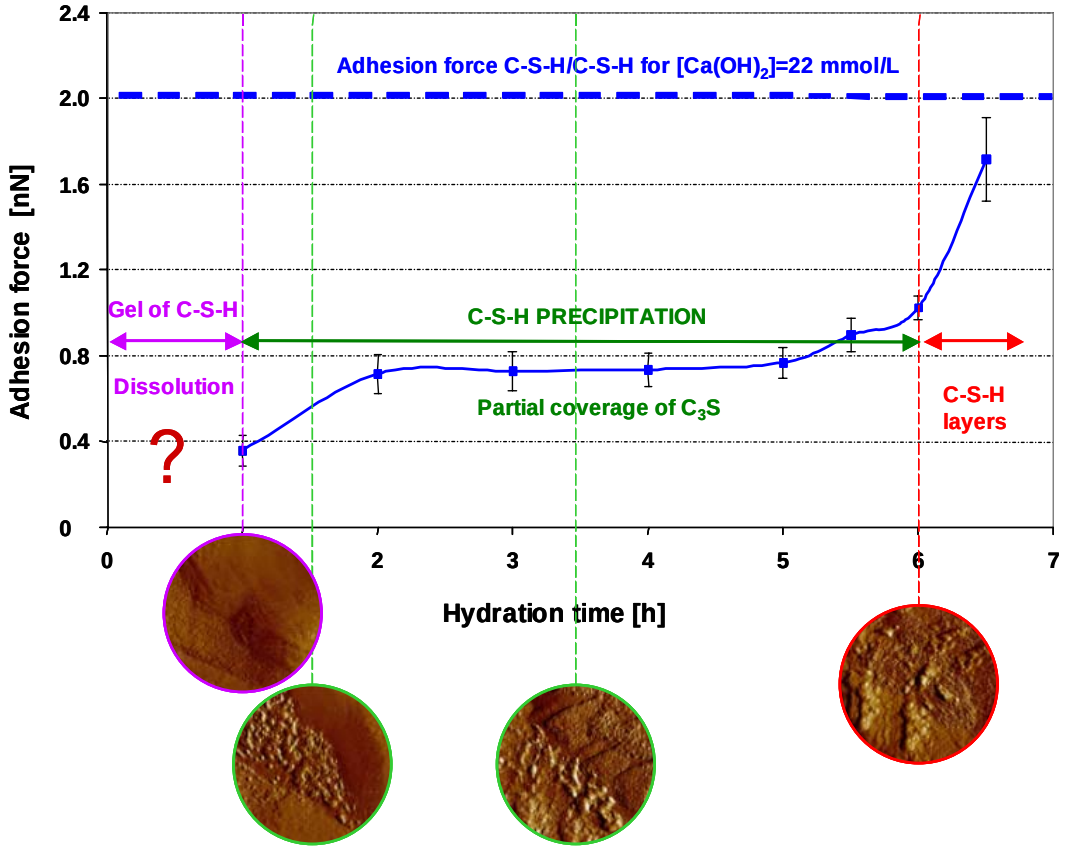

Figure 1 - Evolution of the adhesion force between C-S-H and C_3S during its hydration in solution calcium hydroxide saturated (22 mmol/L).

The interaction kinetics C-S-H/C_3S during hydration is made up 3 periods:
A first period corresponded to the dissolution period of the C_3S surface. During this time, it was impossible to measure the interactions (permanent fluctuation of the cantilever deflection signal). The first measurements of C-S-H/C_3S interaction were performed at the end of this dissolution period, after 1h, and intervened just before the beginning of intense precipitation of the C-S-H (topographic image surrounded of purple line in figure 1). The mean value of the adhesion force F_{adh} without any precipitation of the C-S-H on the C_3S surface was: F_{adh}*=0.36 ± 0.07 nN.* It was obvious that the C-S-H was not formed directly on the C_3S surface but in the neighbour.
A second period corresponded to the C-S-H precipitation on the C_3S surface (topographic images surrounded of green line in figure 1). It is marked on the curves by practically constant values of adhesion force. This average value constant during 4h of hydration was slightly increased to: F_{adh}*=0.75 ± 0.08 nN*
A third period corresponded to the disordered growth of the C-S-H, appearing perpendicularly to the C_3S surface. The consequence was the formation of several inhomogeneous layers of C-S-H (topographic image surrounded of red line in figure

1). A consequent increase in the adhesion force was noticed. After 6h30, the average interaction values reached an adhesion force of about: F_{adh}=*1.72 ± 0.19 nN*. At this time of the hydration, it is quite obvious that this adhesion force will reach the C-S-H/C-S-H interaction since the C_3S surface was entirely covered with several layers of C-S-H nanoparticles. After 7h, it was difficult to keep the calcium hydroxide solution at the same saturation level and to continue reproducible experiments.
We could notice that the time scale was extended due to the high liquid/solid ratio. The volume of the studied crystal was in all cases less than 1mm^3 compared to the 500 µl of calcium hydroxide solution kept in the AFM liquid cell (the $Ca(OH)_2$ solution in the peristaltic pump circuit to be added).

Hydration of C_2S in calcium hydroxide solution

The figure 2 shows the evolutions of the interactions between C-S-H and C_2S, at the time of its hydration in a saturated calcium hydroxide solution (22 mmol/L).
The kinetics of C_2S hydration (specific volume is similar to the volume of the topography study) in saturated calcium hydroxide solution made it possible to measure the interactions acting between C-S-H and C_2S without growth of the C-S-H on the C_2S surface The dissolution period was important (approximately 7 h). So the average values of the adhesion force of the interactions between C-S-H and C_2S in calcium hydroxide solution was approximatively: F_{adh}=*0.60 ± 0.09 nN*.

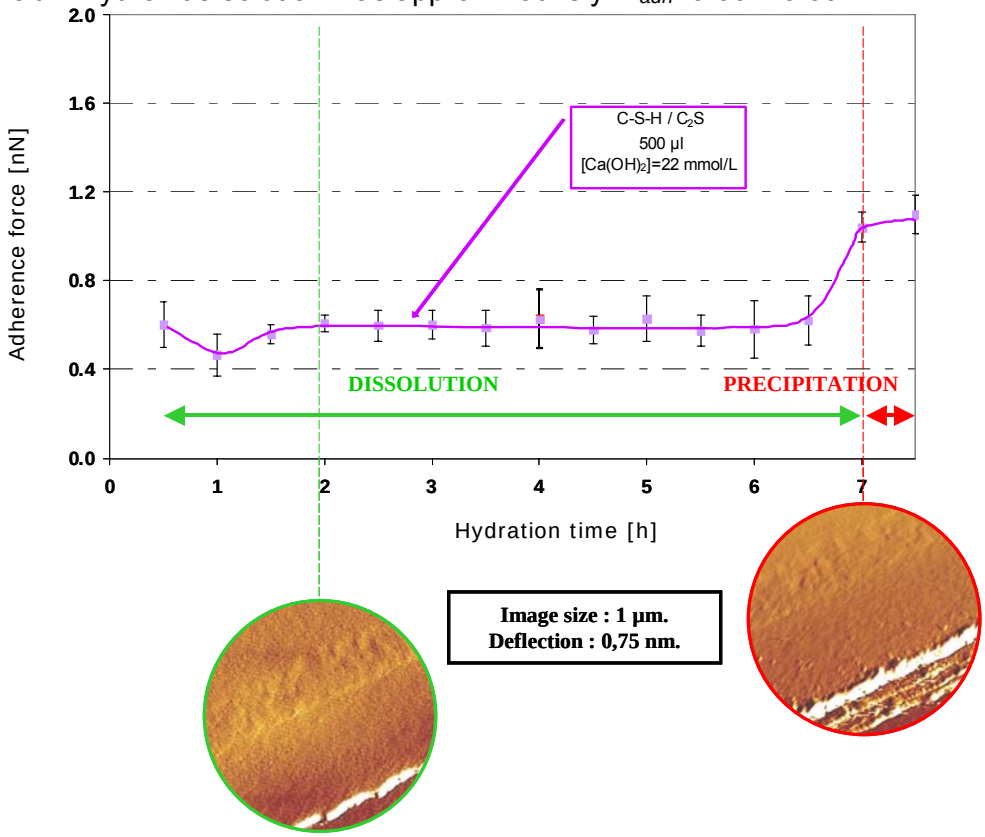

Figure 2 - Evolution of the adhesion force between C-S-H and C_2S during its hydration in saturated calcium hydroxide solution (22 mmol/L).

These kinetics have shown that the beginning of C-S-H precipitation involved an increase in the adhesion force with a value of: F_{adh}=*1.04 ± 0.07 nN*.

During the hydration in saturated calcium hydroxide solution

To study the evolution of the interactions between AH_3 and C_3A during its hydration, several experiments were carried out in saturated calcium hydroxide solution by modifying the specific surface of the C_3A sample in order to analyze the effect of the liquid/solid ratio: surface of 5 x 5 mm^2, 5 x 10 mm^2, and 5 x 15 mm^2 respectively.

For each experiment, the C_3A substrate was immersed in 500 µl of saturated calcium hydroxide solution. With the force curves obtained in various hydration conditions, it was possible to represent the evolutions of the adhesion force according to the hydration time (figure 3). At the beginning of the hydration of C_3A we observed that amorphous phases precipitate rapidly. This gel is AH_3. The topographical analysis and the adhesion force measurements of forces were impossible. After 30 min of the hydration, we noted purely attractive forces, then purely repulsive forces. Lastly, the appearance of a new phase results in an abrupt appearance of purely attractive forces. The three kinetics of hydration showed the same evolution of the adhesion but at different times of hydration. The importance of the specific surface of the substrate, i.e. the liquid/solid ratio, influenced the hydration rate of the C_3A. Smaller the C_3A surface is, more the hydration will be delayed.

The evolutions at the level of the adhesion force also correspond to the changes in the nature of interactions having taken place during the hydration of the C_3A samples. Indeed, at the beginning of each hydration experiment (about 30 min), the interactions were purely attractive and revealed an adhesion force close to 1.4 nN for all C_3A substrates.

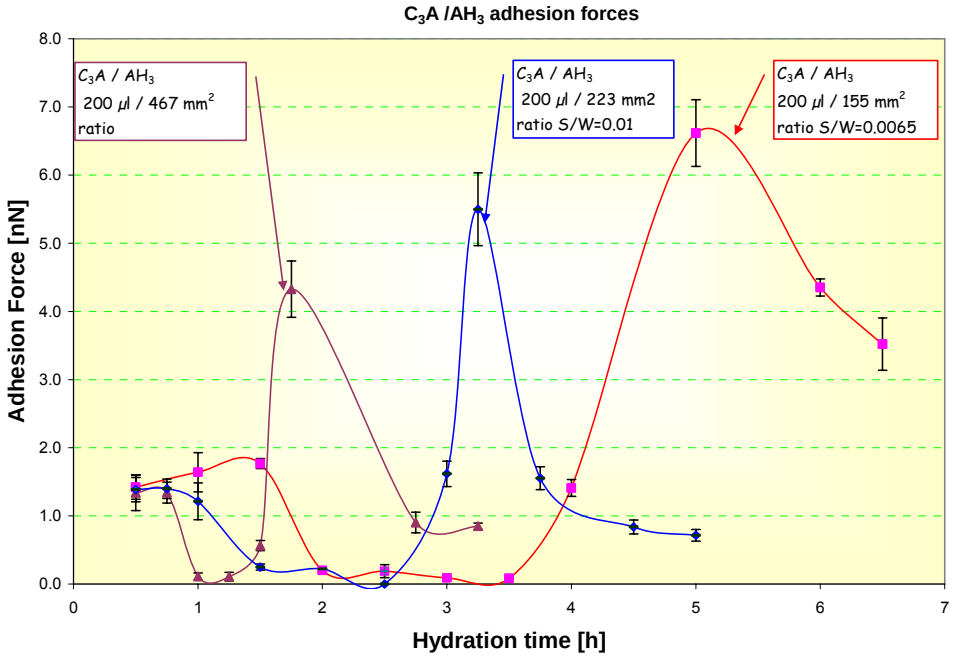

Figure 3 - Evolution of the adhesion force between AH_3 and C_3A during its hydration in saturated calcium hydroxide solution (22 mmol/L). a) surface of C_3A 5 x 15 mm^2 ; b) surface of C_3A 5 x 10 mm^2 ; c) surface of C_3A 5 x 5 mm^2

In all the cases, but at different time, the adhesion force failed but we were always in presence of attractive interactions. However, appeared thereafter, purely repulsive interactions when the adhesion force was remaining practically null. The duration of this repulsive behaviour differs according to specific surface of the sample. This

repulsive period can be explained by the fact that the calcium hydroaluminate C_4AH_{13} precipitated on the C_3A surface tends partially to dissolve.
After a certain repulsive period, the interactions became again purely attractive. It appeared very quickly, an adhesion peak visible in each case, but at different times. This sudden increase of the adhesion was associated with the formation of the solid phase at this time where the calcium hydroaluminates C_2AH_8 and C_4AH_{13} coexists.
After these adhesion peaks, the interactions remained attractive and adhesion values were in agreement with those commonly measured.

3.2 Nanoindentation study

We have measured the Young modulus of different pure cement phases in order to map the profile of polished sections of cement paste hydrated during 10h, 12h, 18h, 24h, 48h, 72h, 7 days, 14 days, and finally 28 days. This mapping will permit to identify the main hydrates and phases, their evolution during the hydration.
The main objectives was the identification of the different phases present in the cement paste, and also to be able to appreciate the mechanical properties of the microstructure according to the location of the nanoindentation probe on the sample. The setup for Young Modulus measurement could be compared to energy dispersive X-ray imaging experiments which accurately identified the concentration of each element at the interface of complex aggregate in cement paste **[12]**.
The average load for indentation was about 500 nN. Two models were used for Young modulus calculation: Hertz model which considers the interaction between an elastic sphere of radius 25 nm and a rigid surface, and the Johnson Kendall Roberts Sperling model which neglects the long range forces outside the contact area and considers only the short range force inside the contact area. To validate the experiments, nanoindentation measurements were performed on green muscovite mica (Mica Co., NY) and foshagite. The results obtained on different C_3S, C_3A, portlandite, ettringite, calcium monosulfoaluminate, and C-S-H samples are summarized in the following table.

Products	Young modulus (GPa)	Error (GPa)
C_3A	130.02	19.14
C_3S	120.78	17.82
Portlandite	108.84	10.67
Ettringite	76.9	12.2
Calcium monosulfoaluminate	96.93	14.3
C-S-H	39.60	10.15

Table 1 – Young modulus of cement phases measured by nanoindentation

Nanoindentation profiles on the cement paste microstructure were carried out. At early age, the impregnation of cement paste by resin created difficulties to analyze the surface (Fig. 4). For each nanoindentation profile, an analysis of 160 force measurement was performed. A typical profile is reported in figure 4.
Polished section of cement paste allows to get rid of the problem of roughness and avoid multiple contacts between nanoindenter and the sample surface.

We have never observed a correlation between the topographic profile and the Young modulus profile (no artefact visible during the acquisition).

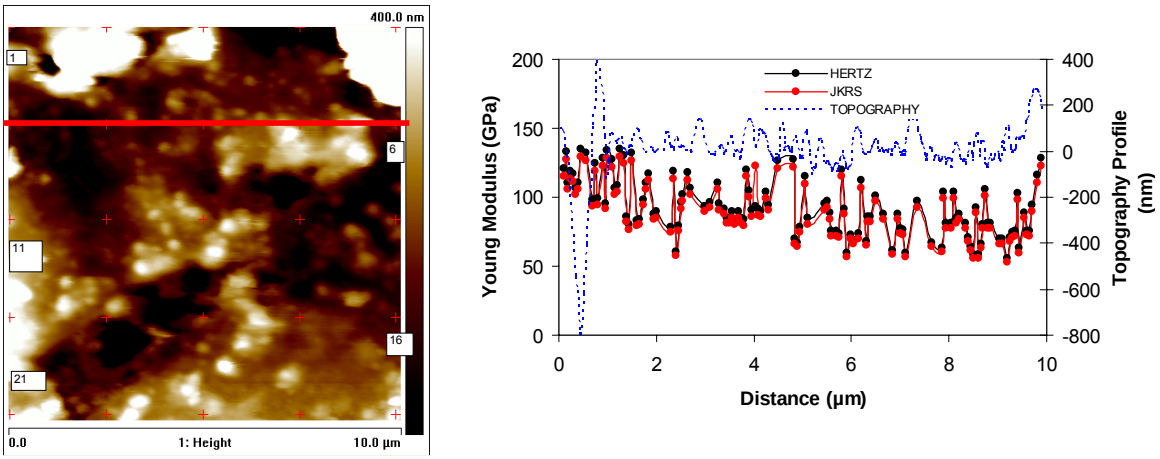

Figure 4 – Young modulus of cement paste composed of alite (80)-C_3A(20)-Gypsum(10) hydrated during 10h. Image range: 10 µm.

Recent experiments allowed differentiation of the anhydrous and hydrate phases. Section profiles by nanoindentation analysis have revealed the evolution of the Young modulus versus the topological location. We have also highlighted that the hydrates resulting from the C_3A hydration had more affinity with alite whereas the hydrates resulting from the hydration of alite had more affinity with tricalcium aluminate. These results allowed to explain the possible rearrangement of the anhydrous grains during the storage of cement and to understand possible affinities of the phases between them which will induce an attraction and strong repulsions between grains. The mechanical properties of anhydrous grains and hydrates resulting from the pure phases studied as a preliminary made it possible to obtain during the measurement of the mechanical properties of a cement paste the evolution of the property on a microscale. This evolution of the mechanical properties showed that the Young modulii of the hydrates observed concerned mostly C-S-H. This Young modulus prevails on the other elastic modulii of the hydrates.

3.3 Nanoconductivity test on C_3A cement phase

The nanoconductivity platinum wire were electrochemically polished in a solution of $CaCl_2$/acetone/water to obtain a probe with an opened angle of about 5° and an active area at the tip apex limited (less than 1000 nm^2). An insulating polymer chemically inert at high pH was used to insulate the two rings of measurement out of platinum (Fig. 5).

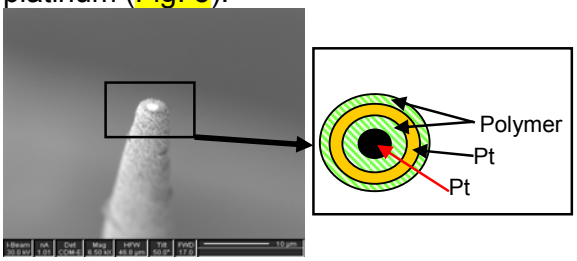

Figure 5 – Nanoconductimetry probe observed by SEM

Calibration of nanoconductimetry probe was performed by measurement of the conductance in an electrolyte standard such as NaCl solution at concentration

C=0.10 mol.L^{-1} to determine the cell constant. Before each measurement, the nanoprobe was rinsed with KCl (50:50) solution and conductivity checked in bi-distilled water.

Then, we have carried out conductivity measurement with the nanoprobe 1 µm above the sample's surface. The approach of the nanoprobe to the alite or C_3A surface was performed using shear force setup **[13]**. In figure 6, we report typical conductance curves measured above alite or C_3A microcrystal. The hydration coincides with the abrupt rise in the conductivity of the alite and C_3A.

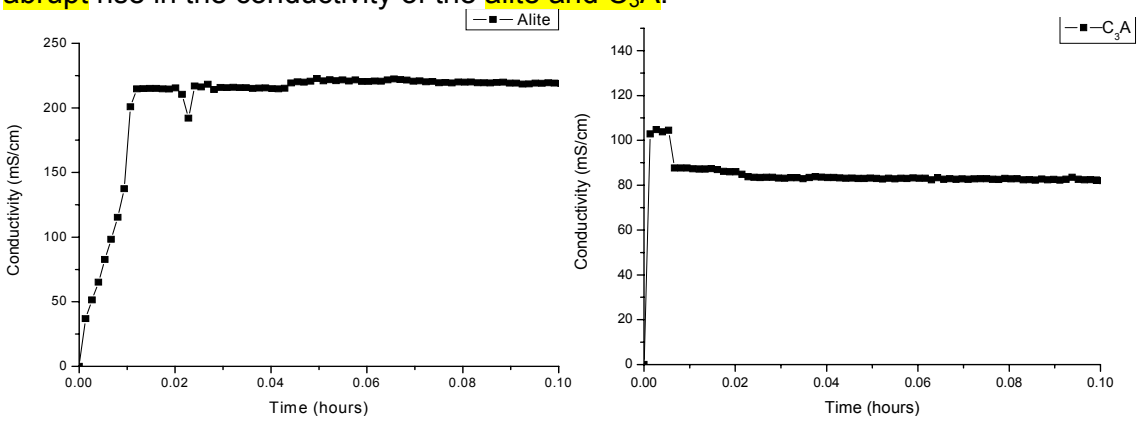

Figure 6 – Nanoconductimetry measurement performed on alite and C_3A

The nanoconductimetry measurements have been performed on the other anhydrous phase C_3S, C_2S. Priority has been done on the reproducibility on nanoprobe fabrication and conductance measurement in reference solution. Mixtures of the different phases, i.e. C_3S-C_3A or C_3S-C_3A-gypsum, were studied in order to characterize the diffusion process in the early age of hydration. We have observed variation of the conductivity during the displacement of the nanoprobe from C_3A surface towards the gypsum surface or from C_3S surface towards the gypsum surface. Depending of time hydration, the motion of the precipitation fronts have been analyzed between C_3S and gypsum grains. The studies have demonstrated that the local conductivity varied in the cement paste with hydration evolution.

4. Conclusion

The present paper describes the experiments based on atomic force microscopy, nanoindentation, and nanoconductimetry. In topography and force volume mode, the AFM makes it possible to correlate the kinetics of hydration on the surface of anhydrous cement phase and the evolution of the cohesion forces within simple systems. In addition, the use of the nanoindentation mode and the use of diamond tip making it possible to limit the probed elastic zone, allows to consider the cartography of the Young modulus, i.e. thevariations of elastic properties directly on the cement microstructure. Lastly, the first conductimetry measurements with a nanoprobe having a submicrometric analysis area dedicated to conductance measurement, associated to a shear force device capable to reach nanometric resolution, make it possible to consider the comprehension of the diffusional processes in the vicinity of surface during the hydration.

References

[1] E. Finot, E. LesniewskaJ.C. Mutin, J.P. Goudonnet,, *Reactivity of gypsum faces according to the relative humidity by scanning force microscopy.* Surface Science 384 (1997) 201-217.
[2] E. Finot, E. Lesniewska, J.C. Mutin, J.P. Goudonnet, *Investigation of surface forces between gypsum microcrystals in air using atomic force microscopy.* Langmuir **16** (2000) 4237-4244.
[3] E. Finot, E. Lesniewska, J.C. Mutin, J.P. Goudonnet, *Investigation of surfaces forces between gypsum crystals in electrolytic solutions using microcantilevers.* J. Chem. Phys. **111** (1999), 6590-6598.
[4] S. Lesko, E. Lesniewska, A. Nonat, J.C. Mutin, J.P. Goudonnet, *Investigation by atomic force microscopy of forces at the origin of cement cohesion*. Ultramicroscopy **86** (2001) 11-21.
[5] C. Plassard, E. Lesniewska, I. Pochard, A. Nonat, *Nanoscale experimental investigation of particle interactions at the origin of the cohesion of cement*. Langmuir 21 (2005) 7263-7270.
[6] C. Plassard, E. Lesniewska, I. Pochard, A. Nonat, *Investigation of the surface structure and elastic properties at the nanoscale of Calcium Silicate Hydrates*. Ultramicroscopy 100 (2004) 331-338.
[7] K.L. Scrivener, *Backscattered electron imaging of cementitious microstructures: understanding and quantification*. Cement and concrete composites 26 (2004) 935-945.
[8] F. Barberon, J.-P. Korb, D. Petit, V. Morin, E. Bermejo, *Probing directly the surface area of a cement-based material by nuclear magnetic relaxation dispersion*, Phys. Rev. Lett. **90**, 116103 (2003).
[9] M.M. Radwan, M. Heikal, Hydration characteristics of tricalcium aluminate phase in mixes containing β-hemihydrate and phosphogypsum, Cem. Conc. Res. 35, 1601-1608 (2005).
[10] M. Regourd, Polymorphisme du silicate tricalcique, C. R. Acad. Sci., Sci. Paris Terre 289, 17– 20 (1979).
[11] R. Maggion, Etude de l'évolution microtexturale de pâtes de silicate tricalcique hydraté, PhD thesis, Univ. of Orléans, 1992.
[12] M.K. Head, N.R. Buenfeld, Measurement of aggregate interfacial porosity in complex, multi-phase aggregate concrete: Binary mask production using backscattered electron, and energy dispersive X-ray images, Cem. Concr. Res. 36 (2006) 337-345.
[13] J.P. Ndobo-Epoy, E. Lesniewska, J.P. Guicquero, *Shear Force Microscopy with a nanoscale resolution*, Ultramicroscopy 103 (2005) 229-236.